Earthq Eng & Eng Vib (2016) 15: 579-595 **DOI**:10.1007/s11803-016-0350-0

Large-scale seismic isolation through regulated liquefaction: a feasibility study

Seyed Amin Mousavi[1†], Morteza Bastami[2‡] and Seyed Mehdi Zahrai[3§]

1. *School of Civil Engineering, College of Engineering, University of Tehran, Tehran, Iran*
2. *International Institute of Earthquake Engineering and Seismology, Tehran, Iran*
3. *Center of Excellence for Engineering and Management of Civil Infrastructures, School of Civil Engineering, Faculty of Engineering, University of Tehran, Tehran, Iran*

Abstract: Using controlled liquefaction, a seismic isolation technique is introduced by which a large area with dozens of structures can be seismically isolated. The proposed Large Scale Seismic Isolation (LSSI) is in many ways similar to conventional base isolations. The required bearing is provided by a fully undrained pre-saturated liquefiable layer which has substantial vertical stiffness/capacity and minimal lateral stiffness. Moreover, required energy dissipation would be provided through material damping and Biot flow-induced damping within the liquefied layer. LSSI consists of a thick non-liquefiable crust layer and an underlying engineered pre-saturated liquefiable layer bounded by two impermeable thin clay layers. The liquefiable layer should be designed to trigger liquefaction as soon as possible within the early seconds of a design level seismic event. Adopting the energy-based GMP liquefaction theory, optimum gradation of the liquefiable layer is also investigated. It turned out that LSSI would effectively reduce acceleration response spectrum within short to medium periods. Contribution of the proposed LSSI is more pronounced in the case of stronger ground motions such as near field events as well as ground motions with longer return periods.

Keywords: liquefaction; seismic isolation; effective stress analysis; ground response analysis; passive control

1 Introduction

Over the past 40 years or so, substantial efforts have been devoted to seismic protection of civil engineering structures. In general, there are two major philosophies in seismic resistant design, namely capacity enhancement and demand reduction. The former technique, which is the dominant current practice, is achieved through implementing lateral strength, stiffness, ductility (energy dissipation), and redundancy in the structure. Meanwhile, in the latter one, the main intention is to reduce imposed seismic demands on the structures using seismic isolation or variable stiffness mechanisms.

Current seismic provisions have aimed to result in a structure with substantial energy dissipation capability. Moreover, the so called energy dissipation could also be achieved by additional energy dissipation devices as well as vibration absorbers (Soong and Dargush, 1997).

Similar to capacity improvement, demand reduction techniques are also achievable through many isolation bearings, such as elastomeric (Yamamoto *et al*., 2009), sliding or friction pendulum (Lu *et al*., 2004), wire rope (Demetriades *et al*., 1993), etc. The main contribution of all isolating techniques is to elongate fundamental period of the isolated structure and change its fundamental eigenvector (mode shape) to resemble a rather rigid body motion. A brief discussion about seismic isolation is provided by Kelly (1996).

Most of the aforementioned seismic protection approaches are concerned only with a single structure. Considering a power plant with a package of infrastructures and facilities, conventional seismic protection techniques should be implemented to all structures in the plant one by one. However, there are some limited efforts devoted to seismic barriers to introduce a larger scale seismic protection. Note that, the term "seismic barrier" differs with "seismic buffers" which have been successfully used to reduce seismic induced soil thrusts on rigid retaining walls (Zarnani and Bathurst, 2009). Seismic barriers (also called seismic screening), are filled or unfilled trenches placed near or around the intended zone, or structure, aimed to disturb propagation of seismic waves through reflection, refraction, dissipation, etc (Woods, 1968; Beskos *et al*., 1986: Leilei, 2012; Shirvastava and Kameswara, 2002).

Correspondence to: Seyed Mehdi Zahrai, School of Civil Engineering, University of Tehran, 16th Azar St., Enghelab Sq., Tehran, Iran
Tel: +98-9192977477
E-mail: mzahrai@ut.ac.ir
†PhD Candidate; ‡Associate Professor; §Professor
Received March 5, 2015; **Accepted** December 20, 2015

While this simple technique leads to encouraging results for high frequency surface waves, such as traffic induced waves, it failed to provide noticeable effect against body wave or lower frequency surface waves with large wavelengths. This is mainly due to the fact that, even in the absence of body waves, depth of the seismic barrier trenches should be in the order of dominant wavelengths of surface waves. Dominant frequencies of design level seismic waves are commonly in the range of 1−10 Hz with average shear wave velocities in the range of 200−400 m/s (in the upper soil layers). Considering the average value of both dominant frequency and shear wave velocity, required trench depth should be at least in the order of 60 m (penetration depth of the surface wave) which is far from feasibility and cost effectiveness. Besides, seismic barriers are mainly effective against surface waves and as suggested by Woods (1968), trench barriers could even amplify seismic waves in the neighboring regions of the isolated zone.

It is well recognized that seismic performance of a given structure is not solely dominated by its structural features. Profound effect of geotechnical features and soil response on the severity and distribution of earthquake induced damages have been reported in many studies. There are some classical examples about soil related damages. The 1985 Mexico City earthquake proved that an earthquake with distance of 350 km can be devastating with the death toll of 10,000 people due to the so called soil amplification. Further case histories about soil related damages have been reported by Naeim (2001), Huang and Jiang (2010), and Huang and Yu (2013). Accordingly, any seismic design without adequate geotechnical consideration might fail to provide reliable seismic protection. In this regard, one interesting point of view is to consider the underlying soil layers as a shear frame and assume that above ground structures were in fact installed on the roof of the imaginary soil shear frame, as shown in Fig. 1. Achieved imaginary dual soil-solid structure is not new concept and has been used in many ground response analysis tools including, SHAKE91 (Schnabel *et al*., 1972), DEEPSOIL (Hashash, 2012), SUMDES (Li *et al*., 1992), and OpenSees (Mazzoni *et al*., 2007). Note that in the case of 2-D and 3-D wave propagation, seismic waves can be imposed both on stories and foundation levels of the dual soil-solid structure. Detailed discussion about above mentioned software has been provided by Stewart *et al*. (2008).

Adopting the dual soil-solid model, all previous seismic protection techniques, namely capacity enhancement and demand reduction, can be implemented on any story of the obtained dual structure. However, there are some differences between seismic protection of conventional frames and that of the dual soil-solid frame. The first, and the most obvious, difference is that all treatments should be implemented at or close to the roof level of the dual soil-solid frame as lower levels correspond to deeper soil layers which are not easily accessible. The second difference is that acceptance criteria should be related to absolute acceleration at the roof rather than roof displacement or inter-story drifts. It is interesting to note that, per current seismic codes such as ASCE 7 (2010), maximum allowable inter-story drift of conventional frames are limited to 2% to 2.5% depending on their fundamental natural frequency. Meanwhile the dual soil-solid frame can sustain much more inter-story drifts in the range of 10% or even more. Note that the inter-story drift in the considered dual frame corresponds to soil shear strain. Earlier studies indicated that both liquefied (Seed *et al*., 2001) and non-liquefied (Kiku and Yoshida, 2000) soils can easily sustain shear strains up to 10%. Even during larger shear strains (up to 60%) hysteretic behavior of the liquefied soil would remain stable (Chiaro *et al*., 2009). However, in such a high strain range, cyclic behavior of the soil would be highly pinched and might be accompanied by soil settlement due to the dilatant nature of the soil medium.

The main scope of the current study is to introduce a Large Scale Seismic Isolation (LSSI) system by which a target zone would be isolated from seismic surface and body waves. Considering the hybrid soil-solid frame, this is done by placing a seismic isolation bearing just below the roof level. The bearing is selected to be an engineered thin pre-saturated liquefiable soil layer through which the roof would be isolated from the lower stories of the dual soil-solid frame. Detailed discussion about the proposed LSSI is represented in the subsequent section.

The basic idea of the current study is not new and some similar base isolations have been proposed in earlier studies. For example, Patil *et al*. (2012) have investigated contribution of sand and geomembrane layers as seismic isolators. They reported average acceleration reductions of 20% to 30% depending on presence of geomembrane layer and water content of the sand layer. In another study, Yegian and Kadakal (2004) proposed a low friction synthetic liner of polyethylene and high strength geotextile as a seismic isolator. Again obtained results were encouraging. However, long term behavior of the proposed synthetic liner and its behavior under wind loads and/or weak ground motions call for

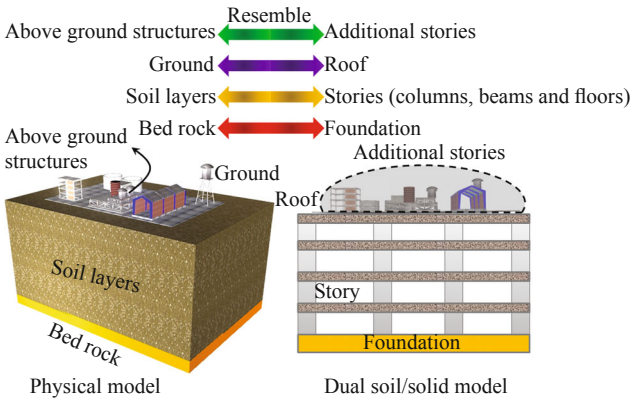

Fig. 1 Dual soil/solid concept

further studies. Dietz and Wood (2006) have proposed an interesting seismic isolation technique in which a caisson-like structure would be penetrated into the soil around the foundation of the main structure. The base of the caisson has a layer with low shear capacity. During a seismic event, this layer would fail and provide a type of isolation for the main structure.

2 Conceptual design of the proposed LSSI

Bearings are the key elements in any seismic isolation technique which should be able to address at least four criteria. That is, low lateral stiffness, high vertical stiffness and strength capacity, some minimal energy dissipation capability, and self-centering. In a large scale view, a fully undrained pre-saturated liquefiable soil layer, as depicted in Fig. 2, would be able to perform similar to a seismic isolation bearing and satisfy above-mentioned requirements. It is crucial to note that the liquefiable layer must be placed in a level surface with minimal slope to avoid pore pressure localization.

2.1 Lateral stiffness

During liquefaction, effective shear modulus and subsequently shear stiffness of the liquefied soil layer would experience significant fall due to the temporary shear strength loss and generated excessive pore water pressure. In the case of large shear strains, cyclic mobility would occur and the shear strength potentially can increase up to its pre-liquefied value. Either cyclic mobility occurs or no, effective shear stiffness of the liquefied soil layer would be low enough to resemble behavior of the conventional isolation bearings.

2.2 t Vertical strength and stiffness

The capability of the liquefied soil to support gravity loads is a controversial issue. Pore water pressure would simultaneously generate and dissipate, albeit with different speeds, during the liquefaction phenomena. Meanwhile, there are some evidences of ground settlement during liquefaction due to the reconsolidation of the liquefied soil. As suggested by some researchers, such as Seed *et al*. (2001), reconsolidation would occur as a result of pore water pressure dissipation through drainage. According to Kramer (1996), "settlement can occur only as earthquake-induced pore pressures dissipate". The same assumption has also been made by Hashash (2012) in DEEPSOIL software. In DEEPSOIL, for example, Terzaghi 1-D consolidation theory was adopted to simulate dissipation of pore water pressure. Terzaghi theory leads to zero consolidation in the case of fully undrained loading (zero hydraulic conductivity). As a result, in a fully undrained condition, there is no dissipation in the developed pore pressure and subsequently the liquefied soil would experience no reconsolidation or settlement. In this case, the water would not squeeze out and the gravity pressure on the liquefied layer (imposed from the crust layer) would be supported through a combination of residual post-liquefaction strength of the liquefied soil and the developed isotropic pore water pressure. So a fully undrained liquefied soil layer would be able to provide the required vertical strength and stiffness which is deemed to be critical for any seismic isolation bearing. Note that during the earthquake, the upper and the lower clay layers would provide a fully undrained state for the middle liquefiable layer, as shown in Fig. 2.

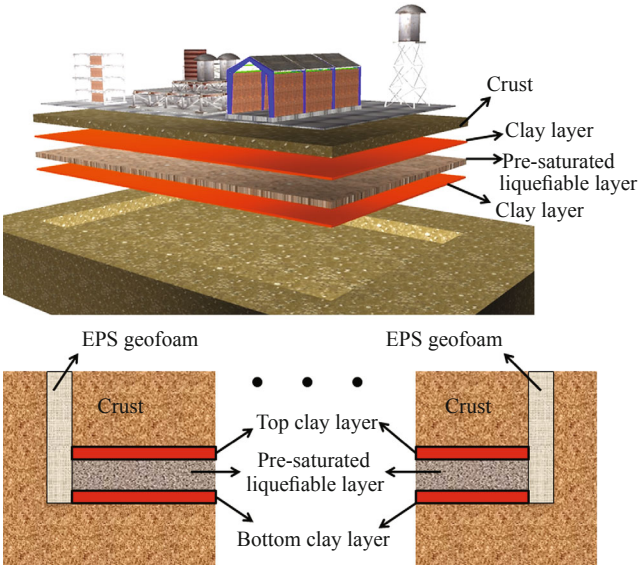

Fig. 2 Main details of the proposed large-scale seismic isolation (LSSI)

2.3 Energy dissipation

Figure 3 shows typical hysteretic behavior of liquefied soils under direct shear test and compare it with that of a typical lead rubber bearing. Note that a lead-rubber bearing is a circular, or sometime rectangular, elastomer with a central lead core. As illustrated in Fig. 3, there is some level of pinching in the behavior of the liquefied soil. While the term "pinching" is widely used by structural/earthquake engineers, it might be ambiguous for geotechnical engineers. Regarding the case of liquefaction, "pinching" refers to cyclic softening and dilatent re-stiffening of the soil. Pinching is generally an undesirable feature in terms of energy dissipation capability and a desirable one with regard to self-centering capability. In any case, according to the current state-of-the-practice some level of pinching is acceptable as cyclic behavior of many seismic resistant systems including reinforced concrete shear walls, un-stiffened steel shear walls, and concentrically braced frames are all, with different levels, pinched.

Note that Fig. 3(b) shows only energy dissipation of the liquefied soil through material nonlinearity (material damping). In a liquefied soil, in addition to material damping, there is another source of energy dissipation from diffusion of pore water or the so called Biot flow-induced damping. As suggested by Bardet (1995) and

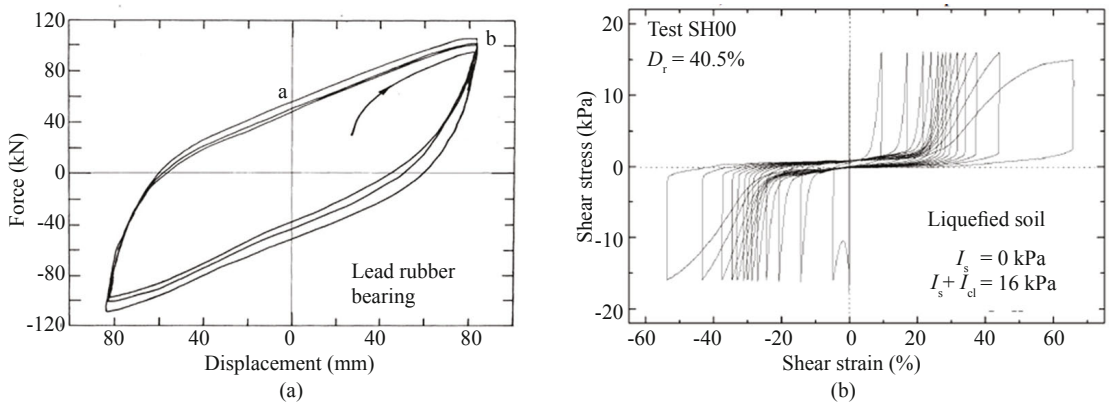

Fig. 3 Comparison between hysteretic behaviors of (a) lead rubber bearing (Robinson and Tucker, 1981) and (b) liquefied soil (Chiaro *et al*., 2009)

Qiu (2010), Biot flow-induced damping could have significant contribution on the overall energy dissipation capability of the saturated granular soils. As a result, substantial level of energy can be dissipated in the liquefied layer of the proposed LSSI.

2.4 Self-centering

Another evolving seismic criterion is self-centering capability of vibrating systems. This is a rather new concept in earthquake engineering motivated by observed excessive post-earthquake residual inter-story drifts in buildings. Most of the current seismic codes have no explicit provision regarding allowable residual deformations, such that self-centering capability of conventional seismic resistant systems dissipating energy at the expense of material nonlinearity is not fully understood. Over the last decade, substantial efforts were devoted to improve self-centering behavior of structural systems. Detailed discussion about this interesting topic is out of scope of the current study and further information can be found elsewhere (Erochko *et al*., 2011). As suggested by Kiggins and Uang a secondary backup elastic system can be effective on self-centering capability of nonlinear systems.

Earlier studies (Athanasopoulos *et al*., 1999) have also shown that EPS geofoams would behave in a rather elastic manner during cyclic loads. As a result, the EPS geofoams which are shown in Fig. 2, can be considered as a secondary elastic system to reduce overall residual displacement of the isolated zone. However residual deformation of a large scale zone might be of less concern.

Apart from self-centering, the main role of the EPS geofoam is to facilitate lateral movement of the isolated zone relative to the un-isolated neighbors and to provide a seismic barrier against high frequency/small wavelength surface waves.

3 Case history observations

Feasibility and efficiency of LSSI concept can be investigated by available ground motion database. This can be done through making comparison between recorded accelerations on liquefied soils and those on non-liquefied soils. Some researchers, such as Miyajima *et al*. (2000) and Kostadinov *et al*. (2000), have focused on this feature and tried to detect liquefied zones from their corresponding recorded ground accelerations. Miyajima *et al*. (2000) observed substantial reduction in horizontal components of the ground acceleration due to the occurred liquefaction. Meanwhile, no noticeable change has been reported with regard to the vertical component. Another important characteristic was reduction of the predominant frequencies of the horizontal accelerations. Obtained results by Miyajima *et al.* (2000) are shown in Fig. 4. Adopting another data base, the same results were obtained by Kostadinov *et al*. (2000). Figure 4 indicates that during liquefaction, horizontal components of the ground acceleration would be decreased while the vertical component remains rather unaffected. Besides, predominant frequencies in liquefied zones are smaller than those of non-liquefied zones. All of these observations would be also the case in any seismic isolation technique.

Reported by Yoshida and IAI (1998), the 1995 Hyogoken-nambu earthquake at the Port Island is another case history for the occurred deamplification in liquefied zones. However, it is crucial to note that delayed liquefaction would fail to contribute to suppression of the surface acceleration. Measured ground acceleration and excess pore water pressure at Wildlife site in 1987 Supersition Hills earthquake clearly proved above claim. In Wildlife site, measured excess pore pressures as well as ground accelerations at different depths indicated that in spite of liquefaction occurrence, surface acceleration has been amplified. The main reason of this peculiar behavior was attributed to delayed liquefaction. In other words, strong pulses of the Supersition Hills earthquake were within the first 15s of the event, while generation of excess pore pressure started after the 15th second. In 2002, Lopez (2002) examined base isolation capability of naturally liquefied soils and concluded that liquefaction does not provide a dependable base-isolation mechanism.

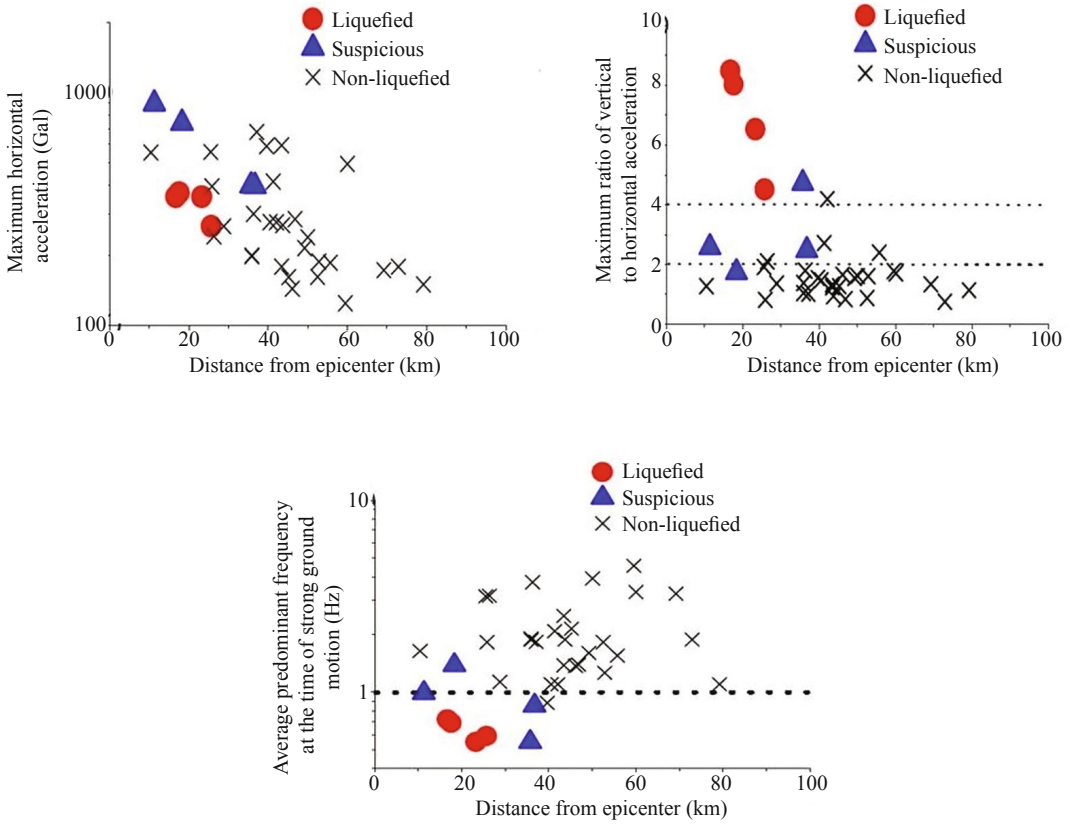

Fig. 4 Measured ground response on liquefied and non-liquefied soils (Miyajima *et al*., 2000)

While this conclusion was based on equivalent linear analyses which are deemed to be inappropriate in the case of liquefiable soils, the authors believe that Lopez's conclusion is reasonable in the cases of natural (un-regulated) liquefied layers. Seismic isolating effects of liquefied soils have been reported in other studies as well (Lopez-Caballero and Modaressi Farahmand-Razavi, 2008; Gosh and Madabhushi, 2003). However, these earlier studies made no attempt to achieve an isolating layer based on liquefaction. This study aimed to reach an engineered liquefiable soil layer to act as a seismic isolating system. As a result, a liquefiable layer should be engineered to trigger fast liquefaction during the early seconds of an earthquake. This would be accomplished by facilitating pore pressure generation and slowing down its corresponding dissipation.

4 Numerical simulation of LSSI

As pointed out in the Introduction section, there are a number of pre-verified numerical tools to perform 1-D to 3-D wave propagation analysis. DEEPSOIL (Hashash 2012), was adopted in the current study due to its ability to explicitly account for nonlinear behavior of soil layers, cyclic pore water pressure generation/dissipation and use of an enhanced frequency-independent multi-mode damping ratio. Soil layers can be modeled with pressure-dependent hyperbolic model as follows (Hashash, 2012; Hashash *et al*., 2010),

$$\tau = \frac{G_0 \gamma}{1 + \beta \left(\frac{\gamma}{\gamma_r} \right)^s} \tag{1}$$

where G_0 and γ are initial shear modulus and shear strain, respectively. Moreover, β and s are two dimensionless curve fitting parameters which would be obtained from the adopted degradation curves (G-γ and D-γ curves). Parameter γ_r stands for the reference shear strain which in contrast with conventional hyperbolic models, was modified to be pressure-dependent through the following formulation,

$$\gamma_r = a \left(\frac{\sigma'_v}{\sigma_{ref}} \right)^b \tag{2}$$

in which effective vertical stress is represented by σ'_v and σ_{ref} is a reference confining pressure with a constant value of 0.18 MPa (Hashash *et al*., 2010). Moreover, a and b are dimensionless parameters which can be obtained from degradation curves. Note that Eq. (2) accounts for dependency of the effective shear modulus (secant shear modulus) on the confining pressure, in an implicit manner. Unloading/reloading model of the soil in DEEPSOIL adopted to follow extended Masing rules through Eq. (3).

$$\tau = \frac{2G_0 \left(\frac{\gamma - \gamma_{rev}}{2} \right)}{1 + \beta \left(\frac{\gamma - \gamma_{rev}}{2\gamma_{rev}} \right)^s} + \tau_{rev} \tag{3}$$

In Eq. (3) γ_{rev} and τ_{rev}, respectively, refer to shear strain and shear stress at reversal points. DEEPSOIL enjoys a reduction factor (R) with which large strain material damping would be reduced for a better agreement with observed experimental results.

$$R = p_1 - p_2\left(1 - \frac{G}{G_0}\right)^{p_3} \tag{4}$$

Note that p_1, p_2, and p_3 are dimensionless curve fitting parameters. It is interesting to point out that, from geomechanical point of view, this reduction in damping stems from dilatant behavior of soil at larger strains and provides a better agreement with experimental results. On the other hand, from structural point of view, reduction of effective damping in higher strains is required due to the pinched behavior of soils within larger shear strains. The same strategy is also the case for reinforced concrete structures, as proposed by FEMA 440 (2005).

The energy-based GMP model (Hashash *et al*., 2010) is used for generation of water pore pressure.

$$r_u = \sqrt{\frac{W_s}{\mathrm{PEC}}} \tag{5}$$

In Eq. (5), r_u stands for the generated excess pore water pressure normalized by effective vertical stress, W_s is density of the dissipated energy (per unit volume) before liquefaction normalized by initial effective confining stress, and PEC (pseudo energy capacity) is a calibration parameter which implicitly accounts for energy dissipation capability of the soil (excluding Biot flow induced damping) before the onset of liquefaction.

Considering only shear deformations, values of W_s and PEC can be estimated by Eqs. (6) and (7), respectively.

$$W_s = \frac{1}{\sigma'_{m0}}\sum_{i=1}^{n-1}\frac{1}{2}(\tau_{i+1} + \tau_i)(\gamma_{i+1} - \gamma_i) \tag{6}$$

$$\ln(\mathrm{PEC}) = \begin{cases} e^{0.0139D_r} - 1.021 & \text{for} \quad FC < 35\% \\ -0.597FC^{0.312} + e^{0.0139D_r} - 1.021 & \text{for} \quad FC > 35\% \end{cases} \tag{7}$$

In Eq. (6) τ and γ denote shear stress and strain, respectively, and the parameter n is number of load increments required to trigger liquefaction. Besides, σ'_{m0} is the initial effective confining stress. In Eq. (7) D_r and FC are relative density and Fines Content (excluding clay) of the soil, respectively. Equation (7) conveys an important feature that should not be overlooked. According to Eq. (7), by increasing the fines content, FC (defined as the percent of dry weight finer than 0.074 mm), the parameter PEC would decrease. As a result, per Eq. (5), for a given level of shear strain, more excess pore pressure would be generated by increasing the fines content. There are some inconsistencies between different studies on the effect of slit content on liquefiable soils and current technology seems to be failed to provide a uniform picture about liquefaction of silty sands and sandy silts. According to earlier case histories, however, silty sand and sandy silt layers with clay contents of less than 15%, are generally susceptible to liquefaction. A brief review of the earlier case histories was reported by Andrews and Martin (2000).

Equations (1) to (7) represent a brief discussion and mathematical formulations aimed to capture nonlinear behavior of dry or saturated cohesionless soils as accurate as possible. This study is based on the presented formulations, while the authors believe that there are still significant uncertainties even in the most advanced liquefaction theories.

In DEEPSOIL, as well as most ground response analysis tools, only one single water table can be defined. However, in the case of LSSI there are actually two separate saturated regions, one bounded within the liquefiable layer of the LSSI and another one bounded by impermeable bed rock and the real water level. As shown in Fig. 5 (a), placing the water table at the top of the liquefiable layer of the LSSI, an equivalent soil profile with a single water table can be defined. In the case of pressure-independent models, the only required modification is to increase pore pressure dissipation in the layers between the LSSI and the real water table. Another alternative is to decrease pore pressure generation in the above mentioned layers. Note that, these layers are actually unsaturated and cannot experience any liquefaction. Validity of the proposed equivalent fully saturated soil profile would be investigated in the subsequent sections.

Another simplification, which is also the common practice, is to impose all related excitations only on the base of the soil column. Figure 5(b) schematically illustrates real excitations which need to be accounted for in an exact site response analysis. While the simplified base-only excitation would fail to cover some features, such as topographical irregularities, high frequency surface waves, etc., it is deemed to be accurate enough for most engineering cases. Note that penetration depth of most surface waves can be quite large depending on their type, propagation velocity, and frequency. For example, penetration depth of a Rayleigh wave propagating in an elastic homogeneous medium at a speed of 200 m/s with 2 Hz frequency would be about 100 m (approximately equal to its wavelength) which is in the order of the whole soil column depth. In other words, parts of the depicted base excitation in Fig. 5 (b) were actually from the surface waves. Due to the fact that LSSI was actually proposed for a large scale zone, effect of boundary conditions of the LSSI, such as EPS geofoams and their backfills, are not explicitly considered in this study. Adopting the presented simplifications, LSSI can be modeled in DEEPSOIL which is deemed to be a practical engineering tool.

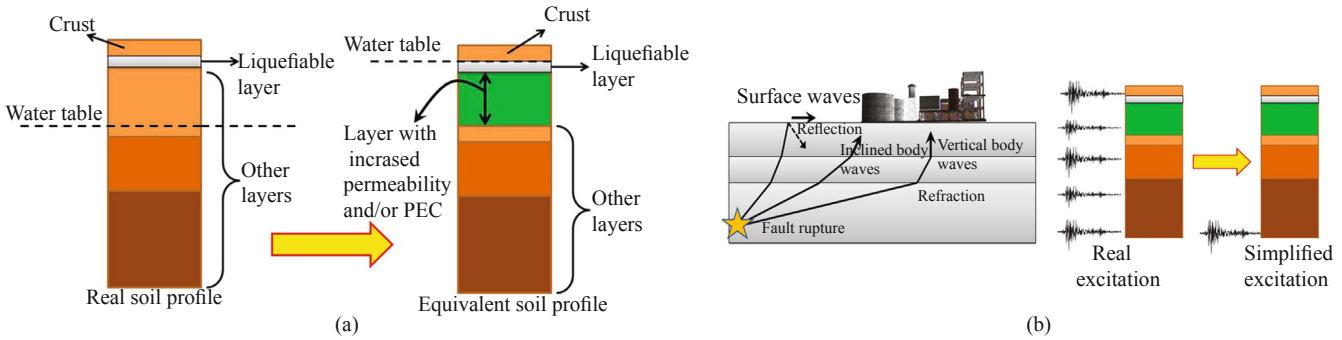

Fig. 5 (a) Equivalent soil profile for LSSI simulation and (b) the simplified base-only excitation

5 Optimum gradation of the liquefiable layer

Gradation and thickness of the liquefiable layer in the LSSI should allow fast liquefaction as well as substantial energy dissipation. These criteria are addressed in the following subsections.

5.1 Fast liquefaction

Liquefiable layer of the LSSI should be designed to be able to trigger liquefaction as soon as possible during the design level seismic event. In other words, excess pore water pressure should be generated fast enough to activate LSSI at the early seconds of the ground motion. Therefore, an optimum liquefiable layer would be obtained by maximizing of the generated pore pressure at a given strain level and minimizing its corresponding dissipation.

$$\text{Maximize}\ (r_u) \equiv \begin{cases} \text{Maximize}\ (W_s) \\ \text{Minimize (PEC)} \end{cases} \equiv \begin{cases} \text{Minimize}\ (G/G_0) \\ \text{Minimize (PEC)} \end{cases} \tag{8}$$

Considering a given shear strain, a well suited index for maximization of the energy dissipation, or equivalently maximizing soil degradation rate, is to decrease $\gamma_{0.5}$ which is corresponding to the shear strain at which $G = 0.5G_0$. As proposed by Menq (2003) $\gamma_{0.5}$ can be estimated as,

$$\gamma_{0.5} = 0.12C_u^{-0.6}\left(\frac{\sigma_0'}{P_a}\right)^{0.5C_u^{-0.15}}, \quad C_u = \frac{D_{60}}{D_{10}} \tag{9}$$

in which, C_u is the so called uniformity coefficient, D_{60} and D_{10} are the grain diameters of 60% and 10% passing (by weight), respectively. Moreover, P_a is the atmospheric pressure equal to 101 kPa. Note that in Menq (2003), $\gamma_{0.5}$ was defined by γ_r and named "reference strain" which is different from that of Eqs. (1) and (2). As a result, in this study the parameter is denoted by $\gamma_{0.5}$ to avoid any ambiguity. Equation (9) indicates that the more the C_u, the smaller the $\gamma_{0.5}$. Therefore, liquefiable layer of the LSSI should have a gradation with large uniformity coefficient. Figure 6 (a) illustrates variation of $\gamma_{0.5}$ with the uniformity coefficient. It is obvious that $\gamma_{0.5}$ has less sensitivity to higher values of C_u (higher than 50).

According to Green *et al*. (2000), the parameter PEC can be minimized through minimizing grain sizes (higher fines contents), minimizing relative density (D_r), and maximizing cyclic stress ratio (CSR). Note that CSR cannot be optimized due to the fact that it depends mainly on the seismicity of the site. In order to monitor sensitivity of the pore pressure generation rate on the aforementioned dominant parameters, a single soil layer is considered as shown in Fig. 7 (a). The layer is fully saturated and its undrained behavior is examined through an increasing harmonic base acceleration. Figures 7 (b), (c), (d), and (e) indicate that contribution of uniformity coefficient (C_u) and fine contents (FC) are more pronounced to reach a fast liquefaction. Accordingly, relatively large C_u and FC should be considered for the liquefiable layer of the LSSI. The authors would like to clarify that the term "fine contents" in this study refers to silt content excluding clay. Bear in mind that many of the above mentioned parameters are correlated to some

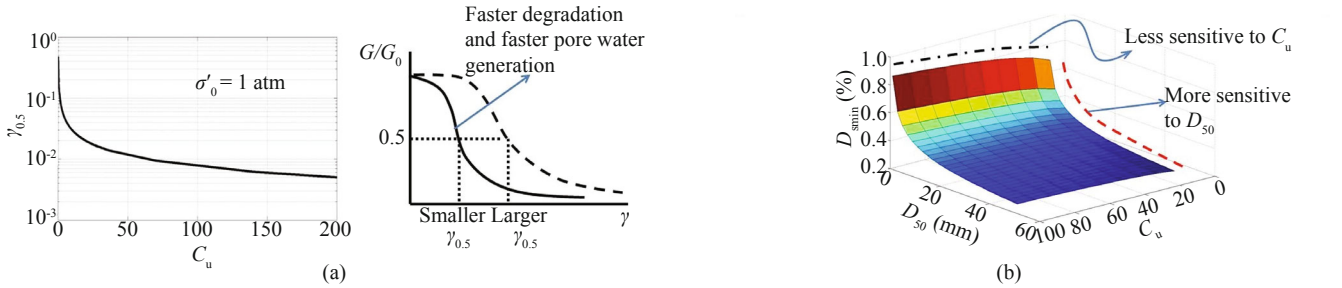

Fig. 6 (a) Contribution of C_u in reducing γ_{50}, and (b) variation of small strain damping ratio with C_u and D_{50}

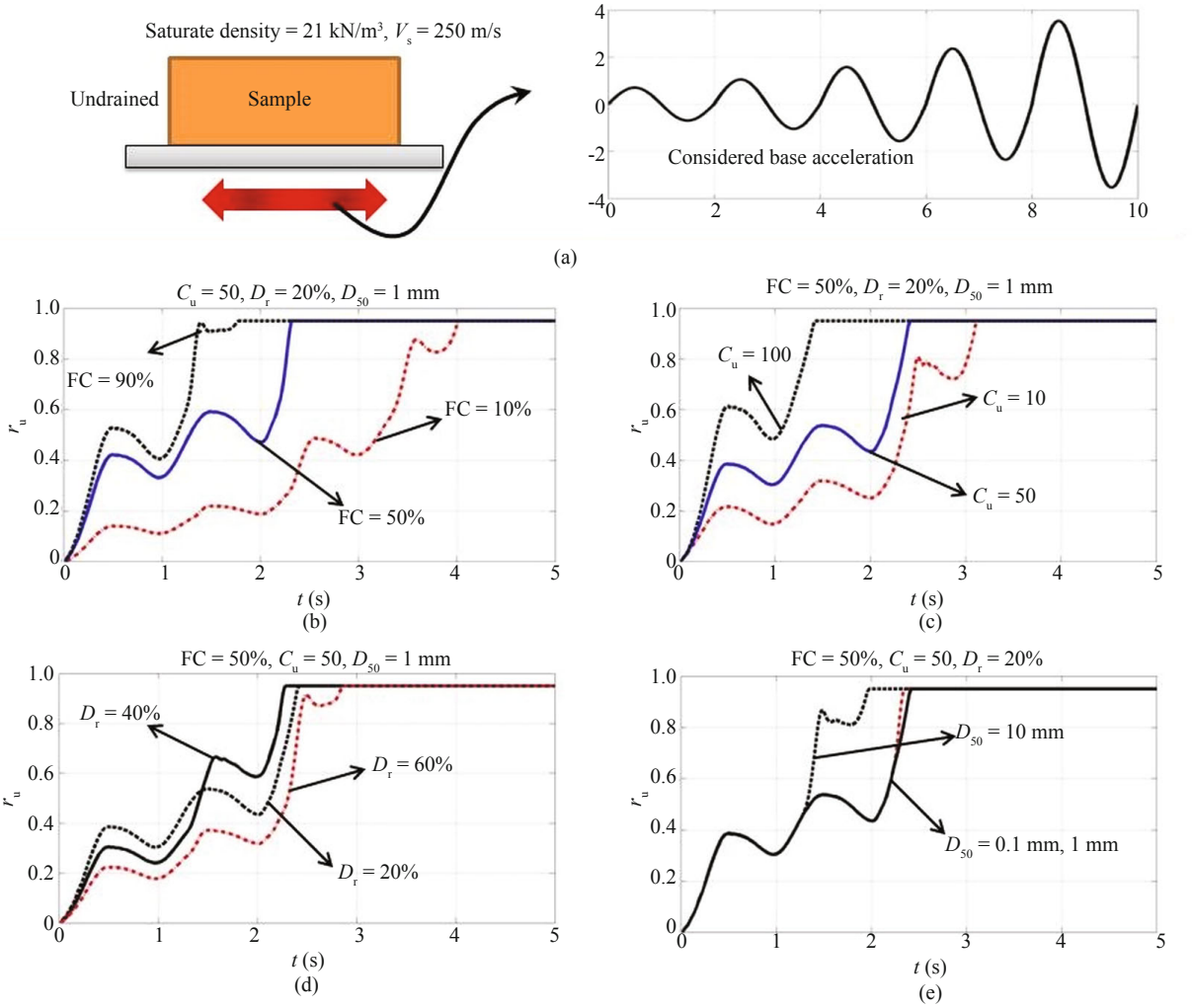

Fig. 7 Contribution of the main parameters in pore pressure generation rate

extent. For example, earlier studies (Menq, 2003) have shown some coupling effects between C_u and maximum/minimum void ratios such that in the case of large C_u (more than 10), maximum and minimum void ratios would remain rather constant with values of 0.45 and 0.2, respectively.

5.2 High energy dissipation

In order to maximize energy dissipation capability of the liquefiable layer in the LSSI, both material damping and initial damping (small strain damping) should be maximized. Material damping (D) was already maximized in the previous subsection through using a high value of C_u (corresponding to small value of $\gamma_{0.5}$). In this subsection, the main focus would be on small strain initial damping, D_{smin}. As proposed by Menq (2003), initial damping can be estimated as,

$$D_{smin} = 0.55 C_u^{0.1} D_{50}^{-0.3} \left(\frac{\sigma_0'}{P_a} \right)^{-0.08} \tag{10}$$

Again the uniformity coefficient, C_u, has an increasing effect on the initial damping. In addition, D_{smin} can be maximized by selecting smaller D_{50} (median grain size in mm). Figure 6(b) illustrates variations of D_{smin} with C_u and D_{50} which clearly shows that liquefiable layer of the LSSI need to have a gradation with small D_{50} This might be impractical, due to the small value of relative density, obtained in the previous subsection. In any case, minimization of the relative density has a much more priority compared with D_{50} as small strain damping has little effect on the overall behavior of the LSSI.

Previous paragraphs were mainly concerned with energy dissipation capability of the soil through material damping. As suggested earlier, however, there is another source of energy dissipation called Biot flow-induced damping which conceptually is very similar to conventional viscous dampers. Flow-induced damping can be substantially increased by increasing viscosity of the saturation fluid. For example, Khan *et al*. (2012) have increased energy dissipation capability of saturated sands by incorporating Bentonite-glycerin mixture in the water. They have observed initial damping ratios as high as 6% which is significantly larger than that of conventional soils (commonly less than 1%). In the current study, however, no effort was made to increase Biot flow-induced damping mainly because these

techniques, according to the current technology, are not seem to be cost effective, especially in a large scale soil medium which is the case in LSSI.

5.3 Thickness of the liquefiable layer

Higher thicknesses of liquefiable layer would increase energy dissipation capability of the proposed LSSI and reduce maximum and residual shear strains within the liquefied layer on one hand. On the other hand, larger thickness would arise significant concerns in terms of tilting stability of the crust layer and calls for excessive excavation. In order to protect the crust layer, its thickness should be substantially larger than that of the liquefied layer. Using earlier case histories, Ishihara (1985) has proposed an empirical relationship between thickness of non-liquefied crust and its underlying liquefied layer, as depicted in Fig. 8 (a). However, these results deemed to be very conservative in the case of LSSI due to the fact that crust layer in the case of LSSI would have enhanced shear strength through engineered gradation and compaction. Possible consequences of thin crust layers are schematically shown in Fig. 8 (b).

The authors would like to note that, comprehensive study regarding to optimum thickness of the liquefiable layer in the LSSI is not feasible through numerical studies. Currently no experimental data is available about this issue and in absence of specific experimental evidences, conservative values of Ishihara (1985), Fig. 8 (a), are deemed to be reasonable.

6 Efficiency of the proposed LSSI

The main scope of this section is to address how and to what extend LSSI would contribute to seismic behavior of structures located on the isolated zone above LSSI.

6.1 Validity of the carried out effective stress analysis

As stated earlier, DEEPSOIL was adopted for the required effective stress analysis in this study. In this subsection, validity of the carried out effective stress analyses are evaluated using the measured data from Wildlife liquefaction array during the 1987 Superstition Hills earthquake. Soil profile and placement of accelerometers and piezometers at the Wildlife site are presented in Table 1 and Fig. 9 (a). Measured accelerations at GL-7.5m was imposed at the base of the modeled soil column and obtained results at the surface are compared with the measured ones. Comprehensive details about the soil layers as well as recorded database of the Wildlife liquefaction array can be found at NEES@UCSB website (http://ness.ucsb.edu).

Illustrated in Fig. 9 (b), it can be seen that DEEPSOIL leads to acceptable results in NS direction. However, it overestimated long period spectral accelerations along EW mainly due to the inherent limitations of 1-D simulations as well as lack of reliable soil parameters. Calculated and measured surface PGAs along different directions are also in good agreement (Fig. 9 (b)).

6.2 Contribution of LSSI on an idealized soil profile

An idealized soil profile is considered which belongs to the site class D, per ASCE 7 (2010), as presented in

Table 1 Soil properties in the wildlife site

Layer	Type	Thickness (m)	γ (kN/m^3)	V_s (m/s)
1	Silty clay	1	15.7	91
2	Silty clay	1.5	19	100
3	Silty sand	4	19.3	130
4	Silty clay	1	19.6	170

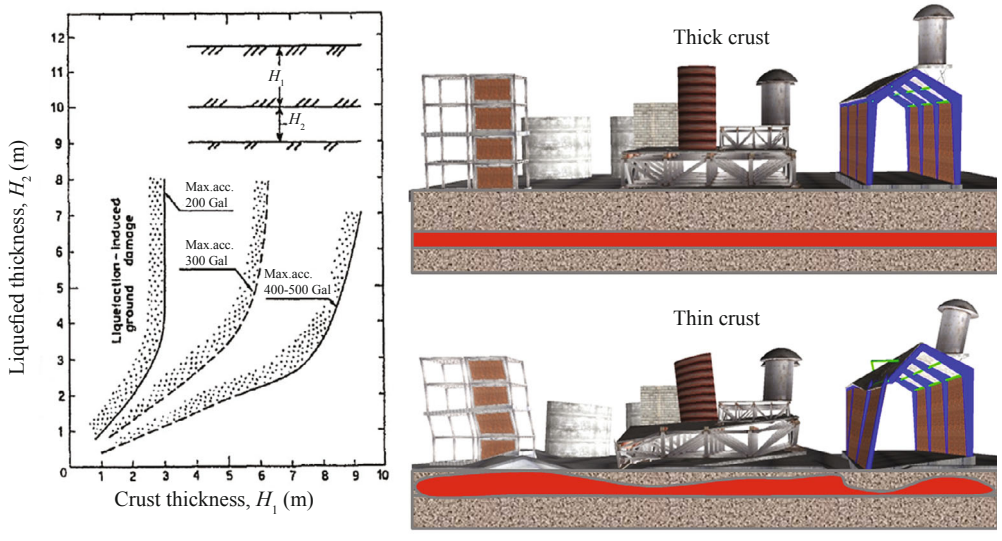

(a) After Ishihara (1985) (b)

Fig. 8 (a) Safe thickness of the crust layer (Ishihara, 1985) and (b) schematic detrimental effect of thin crust layers

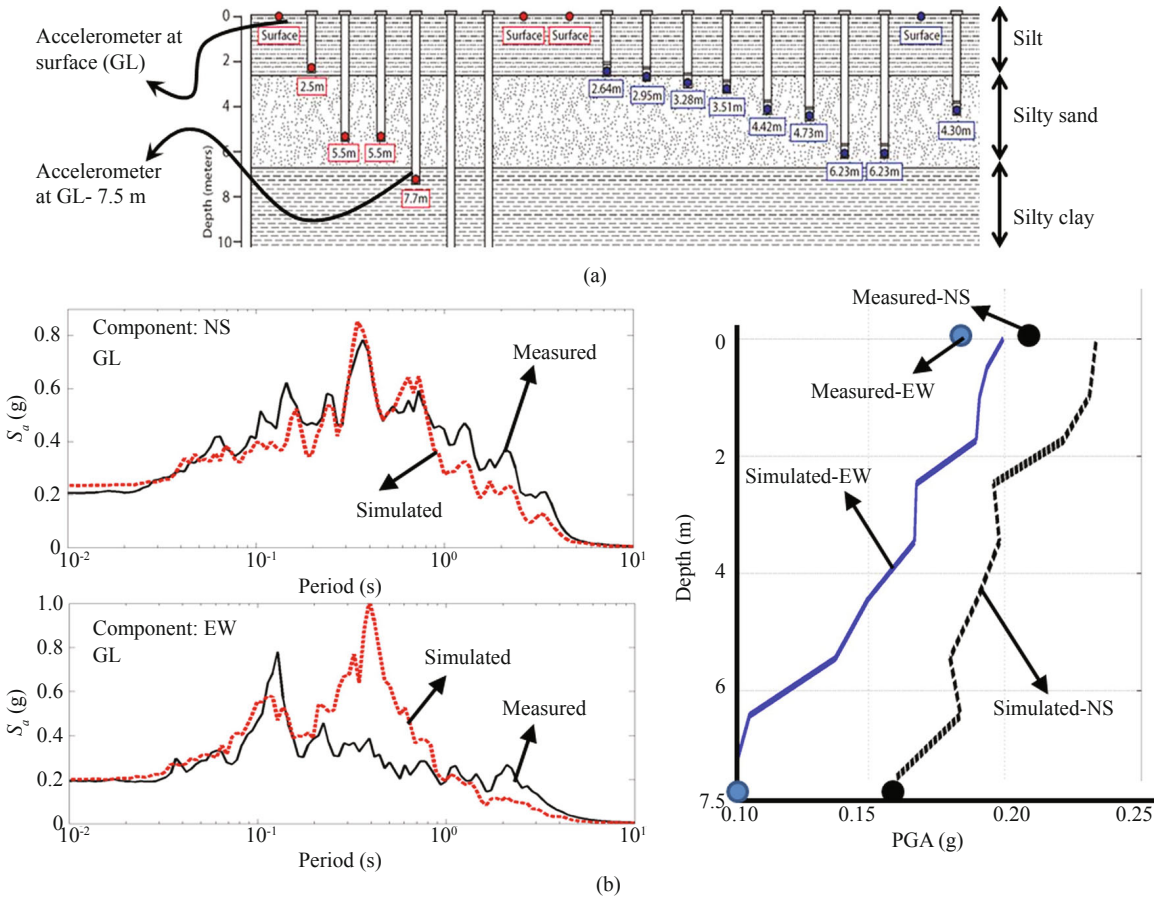

Fig. 9 (a) Schematic view of wildlife liquefaction array and (b) comparison between measured and simulated results

Table 2 Considered soil profile and its equivalent saturated profile

Common properties				Real partial saturated soil				Equivalent full depth saturated soil			
Layer	H (m)	D_r (%)	FC (%)	Water level	γ (kN/m^3)	V_s (m/s)	C_v (m^2/s)	Water level	γ (kN/m^3)	V_s (m/s)	C_v (m^2/s)
1	6	60	15		16	180	1	*	16	180	10
2	6	60	15	*	20	215	1		20	180	1
3	6	75	15		20	260	1		20	225	1
4	6	75	15		21	315	1		21	270	1
5	6	75	15		21	375	1		21	320	1

Table 2. All layers assumed to be silty sand and the mean Seed *et al*. (1986) degradation curve was adopted to be representative for the upper 10 m layers while underlying layers are modeled using the upper limit curves of Seed *et al*. (1986). However, degradation curves of the liquefiable layer of the LSSI were constructed according to the Menq (2003) model which is more refined in terms of soil gradation.

Water table in the real soil profile is located at the depth of 6 m, however in the equivalent profile this level is increased to the ground surface. In the presented assessment, soil behavior is assumed to be pressure-independent and the adopted modification is to increase consolidation coefficient at the artificially saturated layer (Layer 1). Obtained ground response from the introduced equivalent soil profile is compared with that of the real soil profile in Fig. 10 (a).

As shown in Fig. 10 (b), the liquefiable layer of the LSSI would be implemented in a depth of 3m below the ground level. In other words, crust thickness would be 2 m and thickness of 1 m is assumed for the liquefiable layer of the LSSI. Besides, the impermeable clay layers are not included in the modeled soil profile and alternatively a very small value of consolidation coefficient is assigned to the liquefiable layer to simulate its fully undrained behavior. Required parameters of the

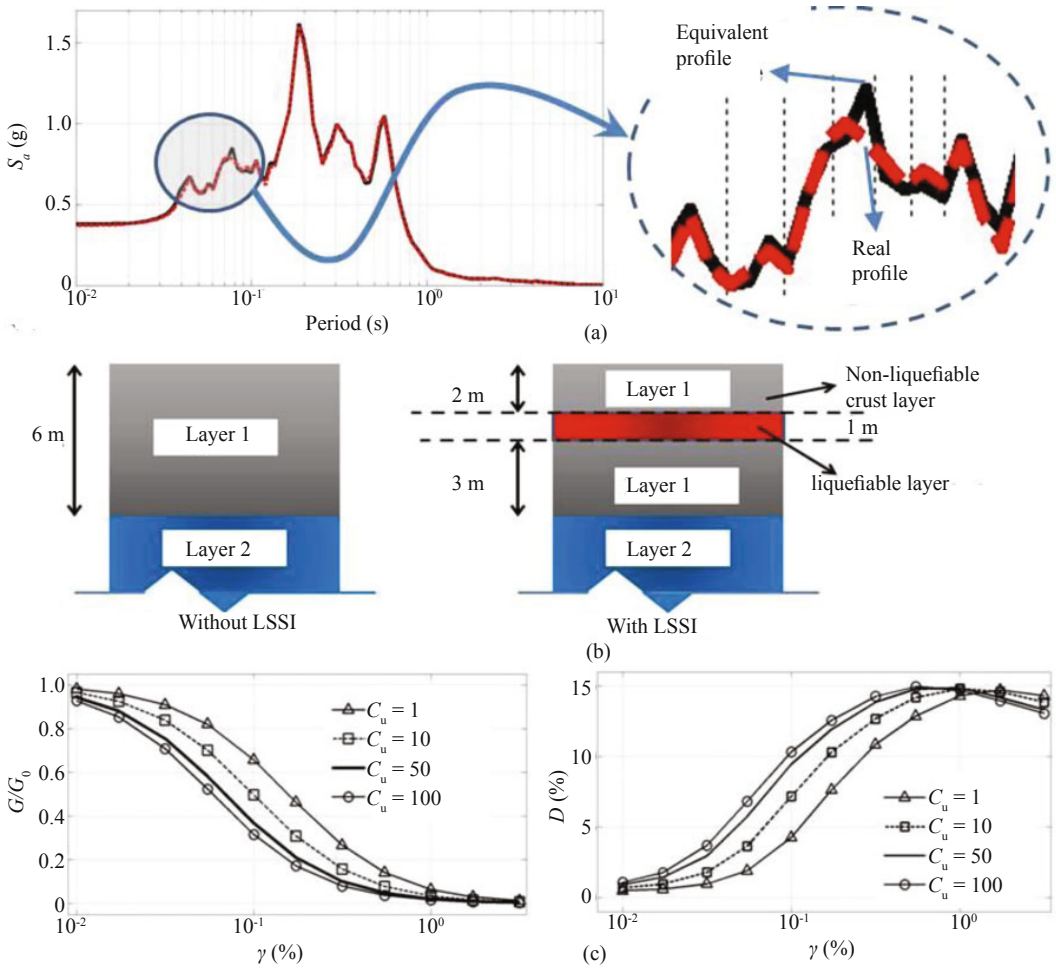

Fig. 10 (a) Validity of the introduced equivalent soil profile, (b) placement of the LSSI, and (c) effect of C_u on degradation curves of the liquefiable layer per Menq's model

liquefiable layer selected to be as follows: $C_u = 50$, $D_{50} = 0.05$ mm, $e = 0.4$, $D_r = 20\%$, FC = 40%, $\gamma = \gamma_{sat} = 21$ kN/m^3, $K_0 = 0.5$, $V_s = 150$ m/s, $C_v = 1\times10^{-4}$ m^2/s where K_0 is the coefficient of at-rest pressure. Many of the above parameters are co-related and care should be exercised to avoid considering unreasonable/impractical parameters for the liquefiable layer. Effects of higher values of uniformity coefficient, C_u, on the Menq's degradation curves are depicted in Fig. 10 (c). As stated earlier, more values of C_u would speed up soil transmission from linear to nonlinear phase, which is a desirable feature for the liquefiable layer of the LSSI.

Kinematic soil-structure interaction is ignored in this numerical assessment. In other words, the effect of the above ground structures on the seismic response of the soil column is ignored and the results reported herein are free-field ground responses. This is a conservative assumption since in most cases, kinematic soil-structure interaction tends to decrease the response at the ground surface (FEMA 440, 2005).

6.2.1 Considered seismic hazard and ground accelerations

Commonly, seismic hazard is defined in terms of its return period, depending on the intended limit states and performance criteria. For example, according to ASCE 7 (2010) return period of design based earthquake (DBE) for conventional buildings is 475 years while this value for typical highway bridges is 1000 years, per ASSHTO (2007). Meanwhile, as stipulated by ASCE 43 (2005), return period of the design earthquake for nuclear facilities varies from 10,000 years to 100,000 years depending on type of the nuclear facility. Due to the page limitation, only two return periods of 475 and 2500 years are considered in this section. The former return period refers to the design based earthquake (DBE) and the latter one refers to the maximum considered earthquake (MCE), per ASCE 7's terminology. Corresponding response spectra are constructed based on ASCE 7 procedure with the following assumptions:

$$S_1 = 0.2 \text{ g, and } S_S = 0.7 \text{ g}$$

where S_1 and S_S are spectral accelerations in periods of 1 s and 0.2 s, respectively, at the outcrop (soil type B). According to ASCE 7, response spectrum of any imposed base ground motion (at bed rock) should be scaled according to 5% damped response spectrum on

the soil type B which can be constructed by S_1 and S_S. Moreover, as the imposed motion is an outcropping one, bed rock of the soil column should be considered to be with finite rigidity. This can be done using the so called Lysmer-Kuhlemeyer (1969) dashpot which is a built-in capability in DEEPSOIL.

Gained from PEER (2013) database, 10 ground motions (5 Far-field and 5 Near-field) were selected and scaled according to the aforementioned technique. Table 3 presents considered seismic events and Fig. 11 shows related scaled response spectra. Adopted records are scaled within the period range of 0.1s to 3s which is deemed to cover most of above ground structures and facilities. Note that only MCE-scale factors are presented in Table 3 as per ASCE 7, DBE-scale factors can be obtained from their MCE counterparts by a reduction factor of 0.67.

6.2.2 Reduction in ground surface response spectrum

Obtained mean results in terms of response spectrum reduction are summarized in Fig. 12 and Table 4. As expected, contribution of LSSI is more pronounced within short to medium periods, e.g. less than 1 s. This characteristic is also the case for conventional seismic isolations.

Figure 13 shows LSSI efficiency in the cases of Far-field and Near-field events. It is clear that LSSI has greater contribution in the case of Near-field ground motions which have higher intensity. The same conclusion can be also made from Fig. 12 by comparing MCE results with those of DBE.

6.2.3 Reduction in ground surface PGA

Deamplification effect of LSSI in terms of PGA is shown in Fig. 14. It is well understood that soil columns would result in less amplification during stronger earthquakes due to the excessive dissipated energy within the soil column. This feature is obvious from Fig. 14 in which MCE hazard level imposed less amplification compared with that of DBE, regardless of LSSI presence. While PGA at the ground surface (or more precisely above the liquefied layer) experienced significant reduction, a rather noticeable jump can be observed in PGA at the layer beneath the LSSI. This observation can be attributed to the low shear strength of the liquefied layer which has provided less constraint for its lower layer.

6.2.4 Maximum and residual strains

Most available experimental data in Soil Dynamics are limited to shear strains less than 20%. Accordingly, this study did not relied upon results corresponding to maximum shear strains of more than 20%. As shown in Fig. 15(a), out of 20 studied ground motions, only 3 have passed this criterion. Note that, obtained results from this 3 ground motions were also excluded from all of the previously presented results. It should be pointed out, however, that flow-type shear strains would never occur in the LSSI due to the presence of geofoam sheets and

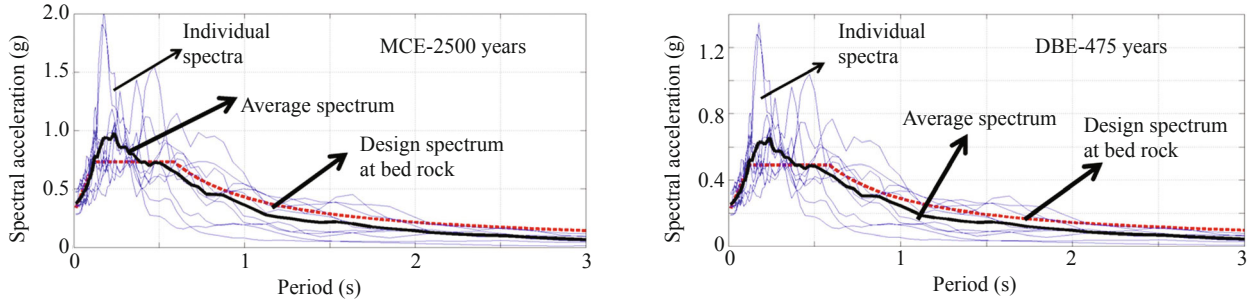

Fig. 11 Spectral accelerations of the scaled ground motions

Table 3 Adopted ground motions

	No.	Event	Station	Comp.	Distance* (km)	Mag.	Un-scaled PGA (g)	MCE-scale factor
Far-field	1	Northridge	Lake Hughes#9	90	26.8	6.7	0.217	2.12
	2	Cape Mendocino	Rio Dell Overpass	270	18.5	7.1	0.385	0.93
	3	San Fernando	Lake Hughes#12	21	20.3	6.6	0.366	1.28
	4	Chi Chi	CHY035	N	18.1	7.6	0.246	1.17
	5	Imperial Valley	Delta	352	43.6	6.5	0.351	0.97
Near-field	6	Kocaeli	Izmit	180	4.8	7.4	0.152	1.84
	7	Northridge	24087 Arleta	90	9.2	6.7	0.344	1.03
	8	Imperial Valley	5054 Bonds Cor.	140	2.5	6.5	0.588	0.63
	9	Parkfield	Cholame#5	85	5.3	6.1	0.442	1.07
	10	Kobe	Nishi-Akashi	0	11.1	6.9	0.509	0.69

* Closest to fault rupture

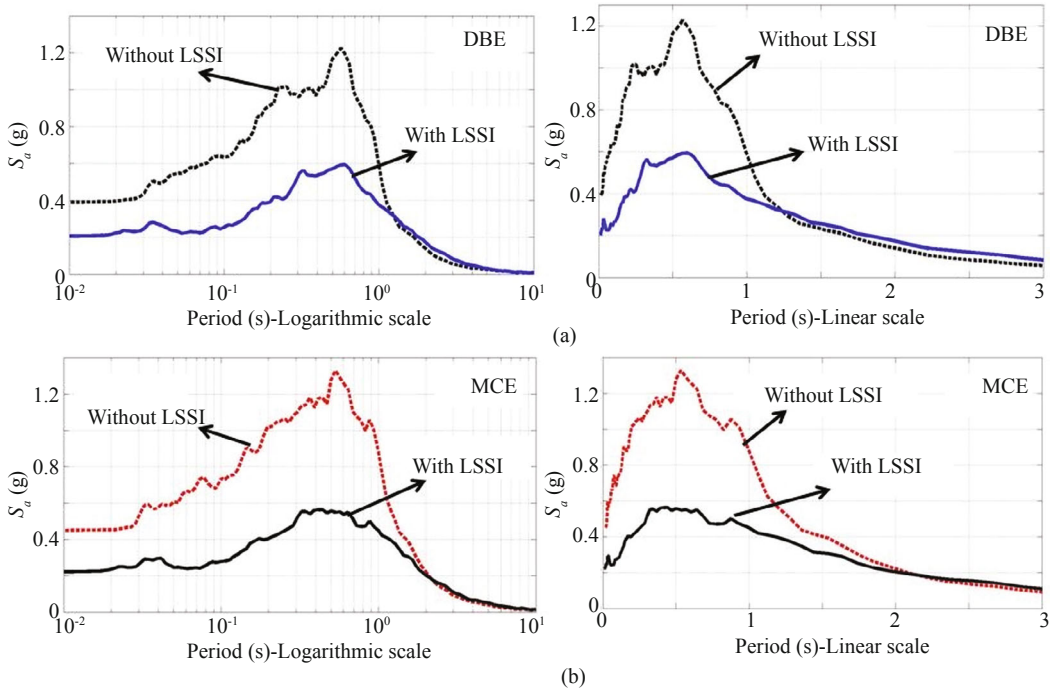

Fig. 12 Reduction in mean acceleration response spectra corresponding to (a) DBE hazard, and (b) MCE hazard

Table 4 Reduction percentage in the average response spectrum

Period (s)	Reduction (%) - DBE	Reduction (%)- MCE
0.2	57	60
0.4	46	52
0.6	50	57
0.8	47	53
1.0	37	49
1.2	5	30

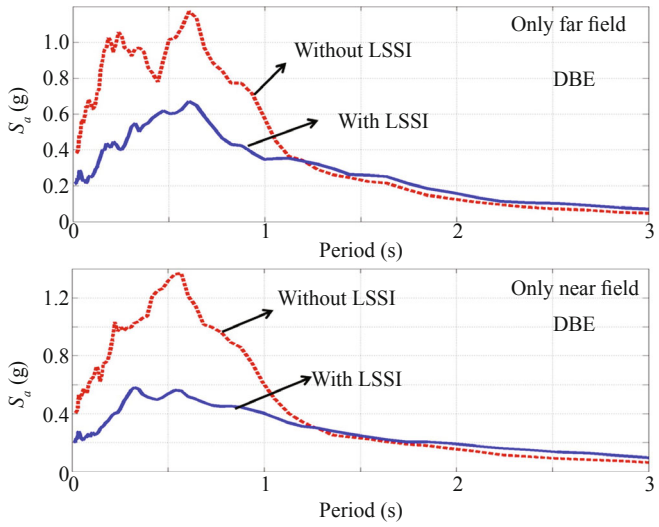

Fig. 13 Contribution of LSSI in far field and near field ground motions

their backfill. Explicit considerations of the boundary conditions provided by geofoam sheets call for 2D or 3D effective stress simulations which are out of scope of the current study.

Three sample hysteresis loops at the liquefied layer of the LSSI are also depicted in Fig. 15 (b). Pinching, stiffness degradation, shear strength degradation, and cyclic mobility are obvious from the obtained loops.

Residual strains in the liquefied layer of the LSSI are presented in Table 5. According to the 1m thickness of the liquefied layer, it can be seen that average residual ground displacement would be 1.6 cm and 2.9 cm in the cases of DBE and MCE hazard levels, respectively. It is crucial to point out that, reported residual strains cannot be generalized in other cases.

6.2.5 Sensitivity to gradation

A parametric study is carried out on the uniformity coefficient of the liquefiable layer. In addition to the previous uniformity coefficient, (C_u=50), three additional values of 25, 75, and 100 are also considered. Note that only ground motions with hazard level of DBE (10%-50 years) are considered in this subsection. From Fig. 16 (a) it can be seen that no improvement would be achieved in the cases of very large uniformity coefficients which are also in agreement with Figure 10 (c). It seems that uniformity coefficients of about 50 to 100 are well suited for the liquefiable layer of the LSSI. Again, regardless of the C_u, LSSI failed to reduce spectral accelerations of larger periods. As schematically depicted in Fig.16 (b), however, this does not mean that

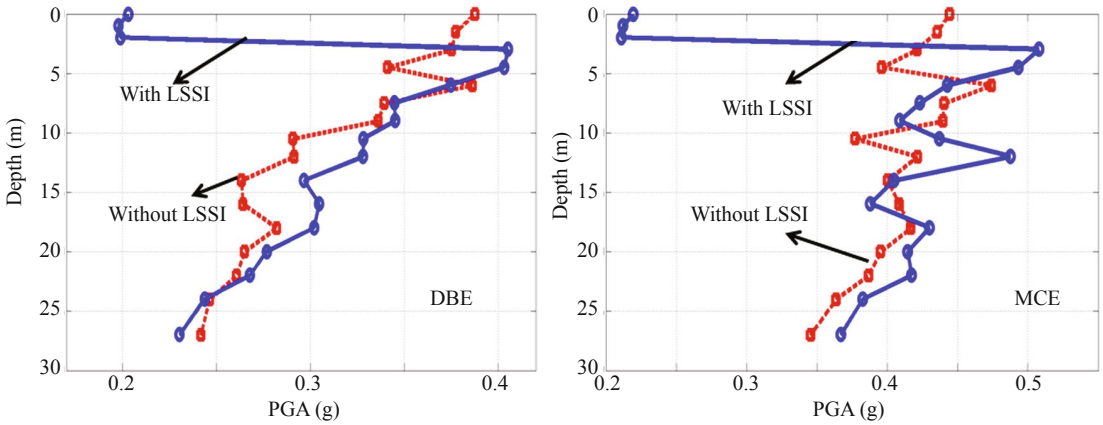

Fig. 14 Variation of PGA along depth of the soil column with and without LSSI

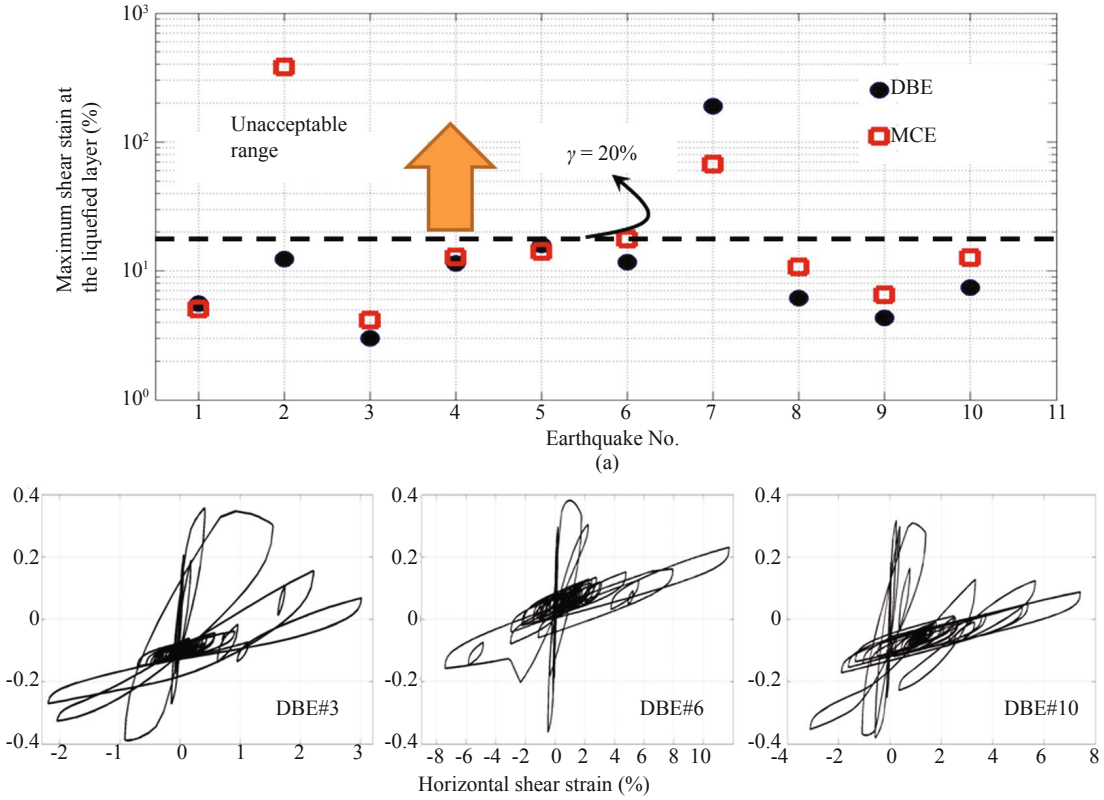

Fig. 15 (a) Maximum shear strains and (b) samples of calculated hysteresis loops in liquefied layer of the LSSI

Table 5 Residual shear strains in the LSSI

Earthquake No.	γ_{res} (%)-DBE	γ_{res} (%)-MCE
1	0.7	0.8
2	3.2	379.6*
3	0.1	0.8
4	0.8	0.6
5	4.6	7.6
6	1.3	2.6
7	189.6*	59.5*
8	0.3	2
9	2.1	2.6
10	1.2	5.9
Average	1.6	2.9

* Excluded

LSSI has no contribution for flexible structures. That is, LSSI would always reduce seismic demands of high frequency modes of vibrations. As a result, considering a flexible structure, LSSI has a noticeable effect on its higher modes which are commonly significant in the case of flexible structures.

Figure 16 (c) indicates that LSSI could reach up to 70% reduction in ground spectral accelerations, depending on the corresponding period of vibration. Maximum shear strains of the liquefiable layer are reported in Fig. 16 (d). Again in most ground motions, maximum shear strains are well below 20% and are rather independent of C_u. Excluding extraordinary shear strains, maximum shear strain in the liquefied layer has a mean value of 9%.

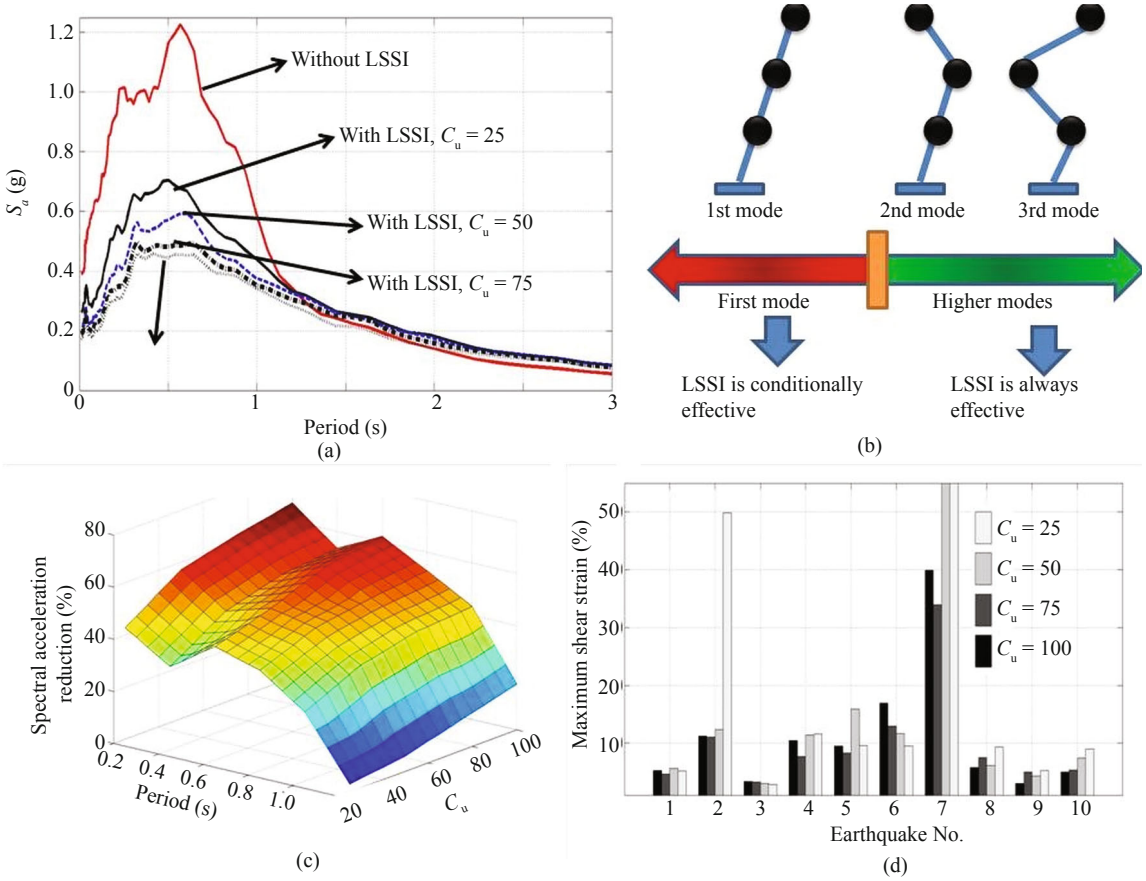

Fig. 16 Sensitivity of the LSSI in terms of (a) ground spectral acceleration, (b) structural modal responses (c) spectral acceleration reduction, and (d) maximum experienced shear strain

7 Conclusion

A Large Scale Seismic Isolation (LSSI) through controlled (engineered) liquefaction was introduced and numerically investigated. In contrast with conventional base isolation, the main intention of LSSI is to isolate a rather large area with dozens of different structures. The main components of the LSSI are the boundary geaofom sheets, non-liquefiable crust layer, upper clay layer, liquefiable layer, and lower clay layer. The liquefiable layer is generally of sandy silt, should be very susceptible to liquefaction, and should generate substantial excessive pore water pressure at the early seconds of ground motions. The main role of the upper and lower clay layers is to avoid/postpone pore pressure dissipation and make the liquefiable layer with minimum shear stiffness and maximum vertical stiffness/strength. The required energy dissipation is provided through material nonlinearity as well as Biot flow-induced damping. Moreover, embedded boundary geofoam sheets act as a seismic barrier against high frequency/ short wavelength surface waves. Geofoam sheets also allow large relative displacements between the isolated zone and its neighboring ground.

Optimum characteristics of the liquefiable layer of the LSSI were investigated using the Menq's model. It is shown that silty sand with high silt content and high uniformity coefficient would be well suited for the liquefiable layer. Adopting a pre-validated 1-D model, contribution of the proposed LSSI is investigated for an ensemble of 10 scaled ground motions with DBE hazard level (10%-50 years) and an additional ensemble of 10 scaled ground motions with MCE hazard level (2%-50 years). The results indicate that LSSI would reduce acceleration spectrum within the short to medium period range, i.e. less than 1s. The contribution of LSSI is more pronounced in stronger ground motions, such as near field ground motions or those with larger return periods (MCE).

Finally, it should be pointed out that LSSI can also be used for a small scale region. However, in this case, boundary condition effects of the geofoams need to be explicitly addressed through 2-D or 3-D simulations. While the idea of LSSI has substantial support from earlier case histories, more studies are still required for a thorough understanding. The authors believes that stability of the non-liquefiable crust against gravity loads, thickness of the liquefied layer, and localization of the generated pore water pressure are among the major concerns which need to be experimentally addressed. Moreover, sensitivity of the LSSI to the soil profile properties (depth, fundamental period, soil type, etc.) is among the important issues for the need further investigation.

References

AASHTO (2007), *AASHTO Guide Specifications for LRFD Seismic Bridge Design,* American Association of Highway and Transportation Officials, Washington, DC.

Andrews DCA and Martin GR (2000), "Criteria for Liquefaction of Silty Soils," *12th World Conference on Earthquake Engineering*, Auckland.

ASCE 7 (2010), *Minimum Design Loads for Buildings and Other Structures*, American Society of Civil Engineers (ASCE), Reston, Virginia.

ASCE 43 (2005), *Seismic Design Criteria for Structures, Systems, and Components in Nuclear Facilities*, American Society of Civil Engineers, Reston, Virginia.

Athanasopoulos GA, Pelekis PC and Xenaki VC (1999), "Dynamic Properties of EPS Geofoam: an Experimental Investigation," *Geosynthetics International*, **6**(3): 171−94.

Bardet JP (1995), "The Damping of Saturated Poroelastic Soils during Steady-state Vibrations," *Applied Mathematics and Computation*, **67**: 3−31.

Beskos DE, Dasgupta B and Vardoulakis IG (1986), "Vibration Isolation Using Open or Filled Trenches, Part1: 2- homogeneous Soil," *Computational Mechanics*, **1**(1): 43−63.

Chiaro G, Kiyota T, De Silva LIN, Sato T and Koseki J (2009), "Extremely Large Post-liquefaction Deformations of Saturated Sand under Cyclic Torsional Shear Loading," *Earthquake Geotechnical Engineering Satellite Conference*, Egypt, pp. 1−10.

Demetriades GF, Constantinou MC and Reinhorn AM (1993), "Study of Wire Rope Systems for Seismic Protection of Equipment in Buildings," *Engineering Structures*, **15**(5): 321−34.

Dietz MS and Wood DM (2006), "Shake Table Testing of a Soft Caisson for Geotechnical Seismic Retrofit," *The 6th International Conference on Physical Modelling in Geotechnics, 6th ICPMG'06*, Hong Kong.

Erochko J, Christopoulos C, Tremblay R and Choi H (2011), "Residual Drift Response of SMRFs and BRB Frames in Steel Buildings Designed According to ASCE 7−05," *Journal of Structural Engineering*, **137**(5): 589−99.

FEMA 440 (2005), *Improvement of Nonlinear Static Seismic Analysis Procedures*, Federal Emergency Management Agency, Washington, DC.

Ghosh B and Madabhusi SPG (2003), "Effects of Localized Soil Inhomogeneity in Modifying Seismic Soil Structure Interaction Effects," *16th ASCE Engineering Mechanics Conference (EM 2003)*, University of Washington, Seattle, USA.

Green RA, Mitchell JK and Polito CP (2000), "An Energy-based Excess Pore Pressure Generation Model for Cohesionless Soils," *Proceedings of the John Booker Memorial Symposium Sydney*, New South Wales, Australia.

Hashash YMA (2012), *DEEPSOIL V 5.1, User Manual and Tutorial*, University of Illinois at Urbana-Champaign, Urbana, Illinois.

Hashash YMA, Phillips C and Groholski DR (2010), "Recent Advances in Non-linear Site Response Analysis," *Fifth International Conference on Recent Advances in Geotechnical Earthquake Engineering and Soil Dynamics and Symposium in Honor of Professor I.M. Idriss*, San Diego, CA.

Huang Y and Jiang X (2010), "Field-observed Phenomena of Seismic Liquefaction and Subsidence during the 2008 Wenchuan Earthquake in China," *Natural Hazards*, **54**(3): 839−850.

Huang Y and Yu m (2013), "Review of Soil Liquefaction Characteristics during Major Earthquakes of the Twenty-first Century," *Natural Hazards*, **65**(3): 2375−2384.

Ishihara K (1985), "Stability of Natural Deposites during Earthquakes," *11th International Conference on Soil Mechanics and Foundation Engineering*, San Francisco, pp. 321−76.

Kelly J (1996), *Earthquake-resistant Design with Rubber,* 2nd ed, Springer-Verlag, London.

Khan Z, El-Emam M, Cascante G and El Naggar H (2012), "Energy Dissipation in Engineered Sand of Large Damping Ratio," *Geomechanics and Geoengineering: An International Journal*, DOI: 10.1080/17486025.2012.695399.

Kiku H and Yoshida N (2000), "Dynamic Deformation Property Tests at Large Strains," *12th World Conference on Earthquake Engineering*, Auckland, New Zealand.

Kostadinov MV, Yamazaki F and Sudo K (2000), "Comparative Study on the Methods for Detection of Liquefaction from Strong Motion Records," *8th ASCE Specialty Conference on Probabilistic Mechanics and Structural Reliability*, University of Notre Dame, IN.

Kramer SL (1996), *Geotechnical Earthquake Engineering*, Prentice-Hall, Upper Saddle River, NJ.

Leilei X (2012), "Influence of In-filled Trench as Wave Barrier on Ground Vibrations," *M.Sc. Thesis*, Royal Institute of Technology, Stockholm.

Li XS, Wangand ZL and Shen CK (1992), *SUMDES: a Nonlinear Procedure for Response Analysis of Horizontally-layered Sites Subjected to Multi-directional Earthquake Loading*, Department of Civil Engineering, University of California at Davis, CA.

Lopez FJ (2002), "Does Liquefaction Protect Overlying Structures from Ground Shaking?," *M.Sc Thesis*, European School of Advanced Studies in Reduction of Seismic Risk, ROSE School, Pavia, Italy.

Lopez-Caballero F and Modaressi Farahmand-Razavi A (2008), "Numerical Simulation of Liquefaction Effects on Seismic SSI," *Soil Dynamics and Earthquake Engineering*, **28**(2): 85−98.

Lu LY, Shih MH and Wu CY (2004), "Near-fault

Seismic Isolation Using Sliding Bearings with Variable Curvatures," *13th World Conference on Earthquake Engineering*, Vancouver, B.C., Canada, Paper No. 3264.

Lysmer J and Kuhlemeyer AM (1969), "Finite Dynamic Model for Infinite Media," *Journal of the Engineering Mechanics Division*, ASCE, **95**: 859−77.

Mazzoni S, McKenna F, Scott MH and Fenves GL (2007), *OpenSees Command Language Manual: Version 2.4.3*, PEER Center, University of California at Berkeley, CA.

Menq FY (2003), "Dynamic Properties of Sandy and Gravelly Soils," *PhD dissertation*, University of Texas at Austin, Austin, Texas.

Miyajima M, Kitaura M and Yamamoto M (2000), "Detection of Soil Liquefaction Using Strong Ground Motion Records," *12th World Conference on Earthquake Engineering*, Auckland.

Naeim F (2001), *The Seismic Design Handbook*, 2nd ed, Springer-Verlag, New York.

Patil SJ, Reddy GR, Shivshankar, Babu R, Jayalaxmi and Binukumar (2012), "Natural Seismic Base Isolation of Structures Having Raft Foundations," *International Journal of Emerging Technology and Advanced Engineering*, **2**(8): 23−38.

PEER (2013), *Strong Ground Motion Database*, http://peer.berkeley.edu/smcat.

Qiu T (2010), "Analytical Solution for Biot Flow-induced Damping in Saturated Soil during Shear Wave Excitations," *Journal of Geotechnical and Geoenvironmental Engineering*, **136**(11): 1501−8.

Robinson WH and Tucker AG (1981), "Test Results for Lead-rubber Bearings for WM.Clayton Building, Toe Toe Bridge and Waiotukupuna Bridge," *Bulletin of the New Zealand National Society for Earthquake Engineering*, **14**(1): 21−33.

Schnabel PB, Lysmer JL and Seed HB (1972), "SHAKE: a Computer Program for Earthquake Response Analysis of Horizontally Layered Sites," *EERC-72/12*, Earthquake Engineering Research Center, Berkeley, CA.

Seed RB, Cetin KO, Moss RES, Kammerer AM, Wu J, Pestana JM and Riemer MF (2001), "Recent Advances in Soil Liquefaction Engineering and Seismic Site Response Evaluation," *Fourth International Conference on Recent Advances in Geotechnical Earthquake Engineering and Soil Dynamics*, San Diego, CA.

Seed HB, Wong RT, Idriss IM and Tokimatsu K (1986), "Moduli and Damping Factors for Dynamic Analysis of Cohesionless Soils," *Journal of Geotechnical Engineering*, **112**(11): 1016−32.

Shirvastava RK and Kameswara Rao NSV (2002), "Response of Soil Media due to Impulse Loads and Isolation Using Trenches," *Soil Dynamics and Earthquake Engineering*, **22**: 695−702.

Soong TT and Dargush GF (1997), *Passive Energy Dissipation Systems in Structural Engineering*, John Wiley, Chichester, UK.

Stewart JP, Lei Kwok AO, Hashash YMA, Matasovic N, Pyke R, Wang Z and Yang Z (2008), "Benchmarking of Nonlinear Geotechnical Ground Response Analysis Procedures," *PEER Report 2008/04*, University of California, Berkeley, CA.

Woods RD (1968), *Screening of Surface Waves in Soils*, University of Michigan, Ann Arbor, Michigan.

Yamamoto S, Kikuchi M, Ueda M and Aiken ID (2009), "A Mechanical Model for Elastomeric Seismic Isolation Bearings Including the Influence of Axial Load," *Earthquake Engineering and Structural Dynamics*, **38**: 157–80.

Yegian MK and Kadakal U (2004), "Foundation Isolation for Seismic Protection Using a Smooth Sysnthetic Liner," *Journal of Geotechnical and Geoenvironmental Engineering*, **130**(11): 1121−30.

Yoshida N and IAI S (1998), "Nonlinear Site Response and Its Evaluation and Presiction," *Proc. 2nd International Symposium on the Effect of Surface Geology on Seismic Motion*, Yokosuka, Japan, pp. 71−90.

Zarnani S and Bathurst RJ (2009), "Numerical Parametric Study of Expanded Polystyrene (EPS) Geofoam Seismic Buffers," *Canadian Geotechnical Journal*, **46**: 318−38.